GB

Institut de Physique Nucléaire de Lyon

Université Claude Bernard

IN2P3 - CNRS

LYCEN 9607
Avril 1996

Configurations of Superdeformed Bands in ^{193}Pb.

L. Ducroux [1], A. Astier[1], R. Duffait[1], Y. Le Coz[1,2], M. Meyer[1], S. Perries[1], N. Redon[1], J.F. Sharpey-Schafer[3,4], A.N. Wilson[3], B.J.P. Gall[5], R. Collatz[6], I. Deloncle[6], F. Hannachi[6], A. Lopez-Martens[6], M.G. Porquet[6], C. Schück[6], F. Azaiez[7], S. Bouneau[7], C. Bourgeois[7], A. Korichi[7], N. Poffé[7,8], H. Sergolle[7], R. Lucas[2], V. Meot[2], I. Hibbert[9] and R. Wadsworth[9]

[1]*IPN Lyon IN2P3/CNRS, Université Claude Bernard,*
F-69622 Villeurbanne Cedex, France
[2]*DAPNIA/SPhN, CE Saclay, 91191 Gif-sur-Yvette Cedex, France*
[3]*Unive of Liverpool, Liverpool L69 3BX, United Kingdom*
[4]*NAC, Faure, ZA-7131 South Africa*
[5]*CRN Strasbourg, IN2P3/CNRS, F-67037 Strasbourg Cedex 2, France*
[6]*CSNSM, IN2P3/CNRS, F-91405 Orsay Campus, France*
[7]*IPN,IN2P3/CNRS, F-91406 Orsay Campus, France*
[8]*Univ. of Oxford, Oxford OX1 3RH, United Kingdom*
[9]*Univ. of York, York YO1 5DD, United Kingdom*

To be published in Phys. Rev C

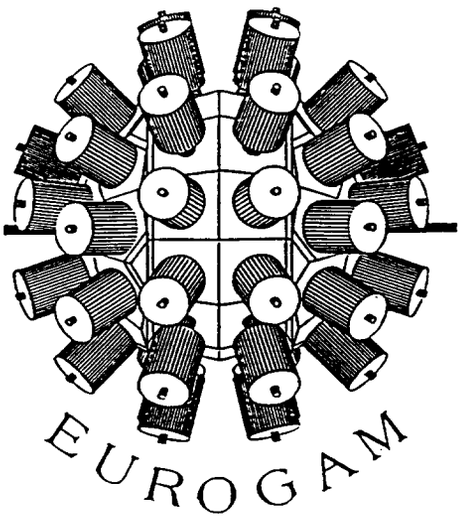

FRANCE - UK
Collaboration

Configurations of Superdeformed Bands in ^{193}Pb.

L. Ducroux, A. Astier, R. Duffait, Y. Le Coz*, M. Meyer, S. Perries, N. Redon
Institut de Physique Nucléaire de Lyon, IN2P3/CNRS,
Université C. Bernard Lyon-1, F-69622 Villeurbanne Cedex, France

J.F. Sharpey-Schafer†, A.N. Wilson
Oliver Lodge Laboratory, University of Liverpool,
PO Box 147, Liverpool L69 3BX, United Kingdom

B.J.P. Gall
Centre de Recherches Nucléaires de Strasbourg, IN2P3/CNRS,
BP 28, F-67037 Strasbourg Cedex 2, France

R. Collatz, I. Deloncle, F. Hannachi, A. Lopez-Martens, M.G. Porquet, C. Schück
Centre de Spectrométrie Nucléaire et de Spectroscopie de Masse, IN2P3/CNRS,
Bât. 104, F-91405 Orsay Campus, France

F. Azaiez, S. Bouneau, C. Bourgeois, A. Korichi, N. Poffé‡, H. Sergolle
Institut de Physique Nucléaire, IN2P3/CNRS,
Bât. 104, F-91406 Orsay Campus, France

R. Lucas, V. Meot
DAPNIA / SPhN, CEA Saclay, 91191 Gif-sur-Yvette Cedex, France

I. Hibbert, R. Wadsworth
Department of Physics, University of York,
Heslington, York YO1 5DD, United Kingdom

Abstract :

The six superdeformed bands in ^{193}Pb have been studied with the EUROGAM 2 γ-ray spectrometer using the $^{168}Er(^{30}Si, 5n)^{193}Pb$ reaction. The results are discussed in terms of Cranked-Hartree-Fock-Bogolioubov-Lipkin-Nogami calculations. From the $\Im^{(2)}$ moment of inertia behaviour as function of the rotational frequency and the M1 and E2 decay competition of the superdeformed states, the bands are interpreted as three pairs of signature partners based on quasineutron excitations. Dipole transitions linking two signature partner superdeformed bands have been observed and, for the first time in lead isotopes, the branching ratio $B(M1)/B(E2) = 0.15 \pm 0.04\, \mu_N^2/e^2b^2$ has been extracted.

PACS number(s): 21.10.Re,21.60.Jz,23.20.Lv,27.80.+w

---

* *present address : DAPNIA / SPhN, CEA Saclay, 91191 Gif-sur-Yvette Cedex, France*
† *present address: National Accelerator Centre, PO Box 72, Faure, ZA-7131 South Africa*
‡ *present address : Department of Physics, University of Oxford, Keble Road, Oxford OX1 3RH, United Kingdom*

I. Introduction

One of the most interesting ways to study the nucleus under extreme conditions of deformation and angular momentum is the observation of superdeformed (SD) states. The existence of SD nuclei has been predicted in the mass A$\sim$ 190 region both by microscopic and macroscopic-microscopic calculations [1 - 5]. Experimentally more than 40 SD bands have been discovered in 20 nuclei [6]. For the lead isotopes, microscopic Hartree-Fock plus BCS calculations [5] have predicted the occurence of a SD well for ^{192}Pb. This nucleus appears as the borderline case of the superdeformation island for the even-even lead isotopes. SD bands have been observed very recently in odd-A Pb nuclei, ^{193,195,197}Pb [7 - 9].

For many SD bands in the mass A$\sim$ 190 region, the dynamical moments of inertia $\Im^{(2)}$ show a typical rise with increasing rotational frequency $\hbar\omega$. This behaviour has been attributed to the alignment of quasiparticle pairs from high-N intruder orbitals in the presence of pairing. However some exceptions remain, in particular two SD bands in odd-A lead nuclei have been observed with approximately constant $\Im^{(2)}$ [7 - 9] such as in ^{192,194}Tl [10, 11] and, at low frequencies, in odd-A mercury isotopes [12, 13]. These "flat" bands have been interpreted in terms of Pauli blocking of quasiparticle alignments in intruder orbitals for odd-A Pb and odd-odd Tl isotopes and, for odd-A Hg isotopes, in terms of occupation of the unfavoured N = 7 neutron orbitals.

Another interesting feature connected to the SD nuclei in the mass A$\sim$ 190 region is the measurement of the magnetic properties. The branching ratios of M1 transitions between signature partner SD bands have been measured for the first time in ^{193}Hg [14] and later in odd proton nuclei ^{195}Tl [15] and ^{193}Tl [16]. Cross talk between SD bands has also been observed in ^{194}Tl [11] and ^{193,195,197}Pb [7 - 9].

In this paper, we report on the new results obtained for the six SD bands observed recently by Hughes et al. [7] in the nucleus ^{193}Pb which is the lightest known odd-A Pb isotope containing SD bands. From the $\Im^{(2)}$ moment of inertia behaviour as function of the rotational frequency and the M1 and E2 decay competition of the SD states, the six bands are interpreted as three pairs of signature partners involving the [761]3/2 $j_{15/2} = 7_2$, [642]3/2 and [624]9/2 neutron orbitals. We have observed the cross-talk transitions between two of these SD bands and, for the first time in lead isotopes, we were able to measure the M1/E2 branching ratio.

II. Experiment

The fusion reaction ^{30}Si + ^{168}Er at beam energy of 159 MeV was used in order to populate high spin states in ^{193}Pb via the 5n evaporation channel. The beam was delivered

by the Vivitron accelerator at the Centre de Recherches Nucléaires in Strasbourg. The experiment was carried out with two self-supporting thin 600 μg.cm^{-2} targets. Gamma rays were detected using the EUROGAM 2 spectrometer [17] which consists of 15 large escape suppressed Ge detectors at backward and forward angles respectively, and 24 escape suppressed "clover" Ge detectors near 90° relative to the beam direction.

Approximately 6×10^8 four- and higher-fold events were recorded on magnetic tapes. After unfolding $\sim 3 \times 10^9$ quadruple coincidences were obtained. 40 % of the events correspond to ^{193}Pb residues. With this reaction we have also populated high spin states in ^{192}Pb (20 % of the events) and we have confirmed the existence of a SD band in this nucleus [18]. We have to note that charged-particle channels α 4n (^{190}Hg) and p 4n (^{193}Tl) are also open in this reaction with the relative yields of ~15 % and ~12 % respectively. The data set has been sorted into different multidimensional spectra (1-D spectra, 2-D matrices, 4-D database). The SD bands have been isolated using directly the triple-gated spectra obtained from four- and higher-fold events and the 4-dimensional DATABASE program [19]. The intensities of the gamma rays have been extracted from double-gated spectra, the background has been substracted according to the method of Crowell et al. [20] modified for an event-by-event reading mode. The algorithm determines, by minimization, the respective weights of single gated and total projection spectra to substract for each pair of a given set of gates.

III. Results and discussion

Analysis of the data first revealed the presence of the six SD bands as reported by Hughes et al. [7] using the ^{174}Yb(^{24}Mg, 5n) reaction with a beam of 131 MeV and the GAMMASPHERE early implementation array (36 detectors). Figure 1 shows triple-gated spectra for the six SD bands found in our data. The relative intensities of the transitions in the SD bands are shown in the insets of Figure 1. The intensities relatively to band 1 are estimated at 0.5, 0.5, 0.5, 0.3, 0.3 for bands 2, 3, 4, 5 and 6 respectively (with the same numbers as Hughes et al. [7]) with a ~20 % uncertainty. Bands 1, 2, 3, 4 and 6 are clearly demonstrated by our quadruple data and are in coincidence with yrast normal deformed transitions in ^{193}Pb [21] such as 881 keV ($17/2^+ \rightarrow 13/2^+$), 520 keV ($21/2^+ \rightarrow 17/2^+$), 593 keV ($25/2^+ \rightarrow 21/2^+$) for bands 3, 4, 5 and 6. Band 1 also strongly feeds the $21/2^-$ state (184 keV transition) and band 2 seems to decay directly to the 881 keV level. Band 5 is strongly contaminated by 5 transitions in the normal deformed level scheme, namely the 213 keV transition (compared to the 213 SD one), 252 keV (254 keV SD), 334 keV (335 keV SD), 413 keV (414 keV SD) and 528 keV (527 keV SD). Therefore the extracted intensities for this band are rather uncertain. Futhermore, to extract this band, we were not able to

use as many gates as for the other bands and band 5 seems less intense than band 6 in Figure 1 whereas their intensities are nearly equal.

Twenty new transitions, over and above those observed by Hughes et al. [7], have been identified in the six SD bands, two at low energies and eighteen at high energies as shown in Table 1. The spin values of the lowest SD states in the bands have been derived according to the method of Becker et al. [22] and Wu et al. [23] : 21/2, 23/2, 17/2 and 19/2 for bands 3, 4, 5 and 6 respectively, and for bands 1 and 2 we adopted the same spin values of Hughes et al. [7] : 27/2 and 17/2. As shown in Figure 1, at low frequency the transition energies of band 3 lie at the midpoint of the corresponding transition energies of band 4, band 5 and 6 present a similar relationship up to the highest observed frequency. As Hughes et al. [7], we suggest that bands 1 - 2, 3 - 4 and 5 - 6 are signature partners.

The experimental $\Im^{(2)}$ dynamical moments of inertia for the six SD bands in ^{193}Pb are plotted in Figure 2 as a function of the rotational frequency, $\hbar\omega$, and for comparison, the $\Im^{(2)}$ for the yrast SD band in ^{192}Pb [18] is also shown. It is clear that bands 3 - 4 and 5 - 6 present the same behaviour as the yrast band of ^{192}Pb with the typical rise from 95 to 115 $\hbar^2/\mathrm{MeV}$ with increasing rotational frequency. However for bands 1 and 2, the dynamical moments of inertia are quite constant as a function of frequency. The experimental routhians for the six SD bands are plotted in Figure 3. The $\mathcal{J}_0$ and $\mathcal{J}_1$ parameters used for the reference are those extracted from a Harris fit to the yrast SD band in ^{192}Pb [18] ($\mathcal{J}_0 = 89.7\,\hbar^2\mathrm{MeV}^{-1}$ and $\mathcal{J}_1 = 104.3\,\hbar^4\mathrm{MeV}^{-3}$). The relative excitation energies for the routhians are governed by the two following assumptions : i) the ordering is consistent with the measured relative population of the bands ; ii) at zero frequency the bands 1 - 2, 3 - 4 and 5 - 6 are degenerate since they are signature partners. Bands 1 - 2 and 5 - 6 show the same behaviour as those given by Hughes et al. [7]. Bands 5 and 6 are degenerate along the whole frequency range but, for bands 3 and 4, with the new transitions we added, a splitting clearly appears at $\hbar\omega \sim 300\,\mathrm{keV}$.

In order to interpret our data, we have extended, for ^{192}Pb, the microscopic Cranked-Hartree-Fock-Bogolioubov calculations with the parametrization SkM* of the Skyrme force using the Lipkin-Nogami prescription for the pairing treatment [24]. These results have been obtained with a seniority force $G_\tau = 12.6\,\mathrm{MeV}$. The neutron single-particle and quasi-particle routhians are plotted in Figure 4a and 4b. As shown in Figure 4a, the valence single-particles available above the Fermi level (λ) are the [642]3/2, [512]5/2, [624]9/2 and below the [640]1/2, [761]3/2 $j_{15/2} = 7_2$ and [505]11/2. For the theoretical quasineutron routhians represented in Figure 4b, at $\hbar\omega = 200\,\mathrm{keV}$, the ordering of the levels is the following : the intruder α = -1/2 [761]3/2 (hole excitation), the two [642]3/2 (parti-

cle excitations), $\alpha = +1/2$ [761]3/2 (hole excitation), the two degenerate [505]11/2 (hole excitations), the two [640]1/2 (hole excitations), the two [512]5/2 (particle excitations) and the two degenerate [624]9/2 (particle excitations). As expected the intruder state 7_2 presents a large splitting. At $\hbar\omega = 0$, all the states between [642]3/2 and [624]9/2 are located within 400 keV. We can compare these microscopic theoretical results to those of the Cranked-Shell-Model (CSM) for an axial deformation of $\beta_2 = 0.478$ and $\beta_4 = 0.07$ of Hughes et al. [7]. In our results, two supplementary low-lying neutron hole excitations, [640]1/2 and [505]11/2, appear and in both calculations the lowest energy orbital is the N = 7, α = -1/2.

For bands 1 and 2, we obtain a good agreement for the routhians between the experimental splitting and the predicted one of the [761]3/2 signatures. This splitting starts at a rotational frequency $\hbar\omega = 50$ keV and reaches a value of 330 keV at $\hbar\omega = 300$ keV. This compares well with the predicted value of 400 keV. It is in fact extremely clear that for frequencies higher than 100 keV this quasiparticle state corresponds to the lowest excitation energy in the HFB spectrum. As expected the corresponding dynamical moment of inertia shown in Figure 2 presents a flat behaviour characteristic of the blocking due to the odd neutron. This pairing blocking effect has already been observed in lead isotopes for bands 1 - 2 in ^{193,195,197}Pb [7-9], in thallium isotopes such as bands 3 - 4 of ^{192}Tl [10], bands 3a - 3b of ^{194}Tl [11] and more recently in ^{191}Hg [13]. So we are agree with the interpretation of these two bands as due to the [761]3/2 intruder N = 7 neutron state as suggested by Hughes et al. [7]. Band 1 is then identified as the favoured partner, α = -1/2, of the [761]3/2 orbital and band 2 the unfavoured one, $\alpha = +1/2$. This assignment is in total agreement with the estimated spin values of 27/2 for band 1 and 17/2 for band 2. We have to note that the spin difference between the normal deformed ground state $13/2^+$ and the estimated spin of the lowest SD state in band 2 is only $2\hbar$. The bump observed in the dynamical moment of inertia for band 2 at $\hbar\omega = 250$ keV could be due to the crossing of the [505]11/2 orbital. In fact, our CHFBLN calculations show an interaction between the N = 7 and N = 5 orbitals, with same parity and same signature, occuring at $\hbar\omega = 250$ keV. Nevertheless, a band which could be a candidate for the other signature partner (α = -1/2) of the [505]11/2 was looked for and was not found.

Concerning bands 3 and 4, with the new observed transitions at high energy, the experimental routhians show clearly a splitting with a strength around 50 keV at $\hbar\omega = 350$ keV. Hughes et al. [7] assigned these bands to the [512]5/2 orbital. In our theoretical scheme, the [642]3/2, [512]5/2, [624]9/2 orbitals are available in particle excitations with increasing excitation energy. The [624]9/2 orbital presents no splitting all along the fre-

quency range. The [642]3/2 and [512]5/2 orbitals display a splitting at $\hbar\omega = 100$ keV and $\hbar\omega = 250$ keV respectively, with a value of 90 keV and 30 keV respectively at $\hbar\omega = 350$ keV. Three points lead us to propose finally for bands 3 and 4 the [642]3/2 assignment at variance with Hughes et al. [7] :

i) the intensities of these two bands are similar to that of band 2; this is in favour of the orbital the closest in energy to the yrast SD favoured band 1 [761]3/2, the ordering of the first predicted levels at $\hbar\omega = 200$ keV being : α = -1/2 [761]3/2, α = -1/2 [642]3/2, $\alpha = +1/2$ [642]3/2, $\alpha = +1/2$ [761]3/2 states;

ii) the energies of the gamma transitions are identical to the ones of bands 2 and 3 in the isotone N = 111 ^{191}Hg interpreted by Carpenter et al. [13] as [642]3/2 in Wood-Saxon calculations. Figure 5 shows the incremental alignments [25] as a function of the rotational frequency for bands 3 - 4 in ^{193}Pb and bands 2 - 3 in ^{191}Hg relative to band 1 in ^{194}Pb and ^{192}Hg respectively. The similar behaviours of these plots reinforce the idea that these bands are due to the same neutron hole added to the two different cores ^{194}Pb and ^{192}Hg;

iii) the last point which is the strongest is that we have observed no M1 cross-talk transitions at low energy linking the proposed signature partners while we do observe such dipole transitions, as will be discussed in the next paragraph for the weaker bands 5 and 6. We have extracted an upper limit of $B(M1)/B(E2) = 0.01\,\mu_N^2/e^2b^2$ for bands 3 and 4. We know that for K = 3/2 bands the calculated B(M1) rates are small ($\sim 0.01\,\mu_N^2$ for spin 23/2) and such linking transitions do not compete with the E2 intraband transitions. On the contrary the B(M1) rates are calculated to be strong for K = 5/2 and K = 9/2 bands (fifty times stronger than for K = 3/2 bands : from 0.47 to $0.77\,\mu_N^2$) and have been measured in ^{193}Hg [14] $B(M1) = 0.81 \pm 0.20\,\mu_N^2$ for the K = 5/2 bands. The lack of cross-talk transitions is corroborated by the facts that we have no strong X-rays (same intensity as for bands 1 and 2) and the intensities of the bands show a plateau before a sharp cut-off.

Of course the experimental splitting occurs at $\hbar\omega = 250$ keV instead of 100 keV in our theoretical cranked HFBLN calculations, as it was the case for ^{193}Hg [24]. This discrepancy could be explained by a small renormalization of the pairing constant. For ^{194}Pb, the calculations of Terasaki et al., [26] using the CHFBLN method predict that the splitting of the [642]3/2 orbital occurs at higher frequency, $\hbar\omega \sim 200$ keV, with pairing correlations described by a zero-range density-dependent interaction instead of $\hbar\omega \sim 150$ keV with a seniority force and there is no change for the other orbitals. So we propose the [642]3/2 assignment for bands 3 and 4 which present a clear splitting and no cross-talk transitions, band 3 (4) being the $\alpha = +1/2$ (-1/2 respectively) partner.

The experimental routhians of bands 5 and 6 present no splitting up to the highest observed frequency. In particle excitations, the [512]5/2 and [624]9/2 predicted orbitals satisfy this condition up to 250 keV and 400 keV respectively. Both configurations must induce large B(M1) cross-talk rates. Figure 6 shows the 213, 252, 295, 336, 375 keV transitions of band 5 on a spectrum gated on band 6 and also, between 100 and 230 keV, 13 cross-talk transitions. The presence of strong X-rays of twice as intense for these two bands compared to the others indicates the presence of relatively highly converted transitions. Figure 7 displays the level scheme for the observed bands 5 and 6 structure. The energy sum rules are fulfilled with a maximum error of 0.5 keV from the cross-talk transitions 100 keV to 221 keV, i.e. up to the 433 keV SD E2 transition ($\hbar\omega = 0.2$ MeV). Up to this point of the discussion two configurations are possible : [512]5/2 and [624]9/2. We have extracted the B(M1)/B(E2) ratios directly from the γ-ray photon M1/E2 branching ratios and we obtain values around $0.15 \pm 0.04\, \mu_N^2/e^2b^2$. The large error is due to the lack of statistics. The absolute B(M1) values have been derived taking into account the theoretical quadrupole moment Q_0 values of ^{192}Pb. In the strong coupling limit the B(M1) value for a $K \neq 1/2$ band can be written :

$$B(M1) = \frac{3}{4\pi}(g_K - g_R)^2 K^2 \langle IK10|I-1K\rangle^2 \qquad (\mu_N^2)$$

$$g_K = g_l + (g_s - g_l)\frac{\langle S_z\rangle}{\Omega}$$

$$\text{and} \quad B(E2) = \frac{5}{16\pi}\langle IK20|I-2K\rangle^2 Q_0^2 \qquad (e^2fm^4)$$

Concerning the Q_0 value, the experimental result for ^{194}Pb is 20 ± 4 eb [27] and the corresponding theoretical values in static HF + BCS calculations using the parametrization SkM* of the Skyrme force [5] are 18.2 eb for ^{194}Pb and 18.4 eb for ^{192}Pb. However in fully self-consistent GCM calculations performed for the even-even lead isotopes series [28], taking into account all the quantal fluctuations associated with the collective variable q_2 related to the axial quadrupole deformation, the existence of a GCM superdeformed state in ^{192}Pb is confirmed at lower excitation energy than in the heavier lead isotopes, but with a smaller quadrupole deformation, $Q_0 = 16.7$ eb. The GCM calculation result for ^{194}Pb, $Q_0 = 18.7$ eb, is in perfect agreement with the experimental value. Figure 8 shows the deduced $(g_K - g_R)K\, f(I,K)/Q_0$ $(f(I,K) = \langle IK10|I-1K\rangle/\langle IK20|I-2K\rangle)$ values for four SD states of band 6 as a function of their evaluated spins. Band 5 was too contaminated to extract the γ-ray photon M1/E2 branching ratios. The theoretical limits for the configurations [512]5/2 and [624]9/2, using $g_s^{\text{eff}} = 0.9\, g_s^{\text{free}}$, are indicated by full lines for the experimental value $Q_0 = 20 \pm 4$ eb of ^{194}Pb, and dotted and dashed lines for the predicted values of ^{192}Pb, $Q_0 = 18.4$ eb and $Q_0 = 16.7$ eb respectively. The data are in agreement with the assignment of the [624]9/2 configuration. This is corroborated by

the fact that the γ-ray energies of these two SD bands and the energies of the linking M1 transitions are identical to those of bands 2b and 3 in ^{193}Hg [14] which have also been interpreted as [642]9/2. This assignment is also in agreement with the calculations of Terasaki et al. [26]. The average $(g_K - g_R)K\, f(I,K)/Q_0$ value was found to be equal to $-0.245 \pm 0.070\,(\mathrm{eb})^{-1}$. So, using the conventional $g_R = \mathrm{Z/A}$ and $Q_0 = 18.4\,\mathrm{eb}$, we obtain for the experimental value $g_K = -0.39 \pm 0.12$. In Table 2 are reported the theoretical values : $\langle \mathrm{s_z} \rangle$, the intrinsic spin on the z-axis, and g_K, for the neutron [512]5/2 and [624]9/2 configurations, extracted from Hartree-Fock + BCS calculations using the parametrizations SkM* [29] and SIII [30] of the Skyrme force, and Woods-Saxon wave functions of Semmes et al. [31]. The first remark is that the microscopic (HF) and the macroscopic-microscopic (WS) approaches are in perfect agreement for these two configurations. The theoretical g_K values can be compared to the two experimental values in ^{193}Hg [14] and ^{193}Pb (this work). The experimental g_K values are in agreement with the predicted ones if one takes $g_s^{\mathrm{eff}} \sim 0.9\, g_s^{\mathrm{free}}$. This assignment for bands 5 and 6 puts a question as regards to the non-observation of the two SD bands corresponding to the quasineutron [512]5/2 configuration. It could be understood if one of these non-observed bands is a pair of identical bands of opposite parity as it is the case for bands 2a and 2b in ^{193}Hg [14]. Our difficulties to isolate band 5, which is strongly contaminated, could explain this non-observation.

IV. Conclusion

The main results of this work are the following : first, the confirmation of the six SD bands discovered by Hughes et al. [7] and the assignment of bands 1 and 2 as due to the [761]3/2 intruder N = 7 neutron state. Second, at variance to the previous work, we proposed the [642]3/2 assignment for bands 3 and 4 which present a clear splitting in the experimental routhians and no cross-talk transitions. Finally, we have observed for the first time in lead isotopes the M1 connecting transitions between bands 5 and 6 and the measurements of the branching ratios that we have extracted from these data lead us to propose for these bands the assignment of the [624]9/2 quasineutron configuration.

Acknowledgements

We would like to thank all those involved in the setting up and commissioning of EUROGAM 2, especially D. Curien, G. Duchêne and G. de France. We are especially indebted to A. Meens of the CRN Strasbourg for manufacturing the targets and the crew of the VIVITRON. We would also like to thank J. Meyer and B. Haas for the numerous interesting discussions. The EUROGAM project is funded jointly by IN2P3 (France) and EPSRC (UK). One of us (ANW) acknowledges the receipt of an EPSRC postgraduate studentship.

References

[1] P. Bonche, S.J. Krieger, P. Quentin, M.S. Weiss, J. Meyer, M. Meyer, N. Redon, H. Flocard and P.-H. Heenen
Nucl. Phys. **A500** (1989) 308.

[2] M. Girod, J.P. Delaroche and J.F. Berger
Phys. Rev. **C38** (1988) 1519.
M. Girod, J.P. Delaroche, D. Gogny and J.F. Berger
Phys. Rev. Lett. **62** (1989) 2452.

[3] R.R. Chasman
Phys. Lett. **B219** (1989) 227.

[4] W. Satula, S. Cwiok, W. Nazarewicz, R. Wyss and A. Johnson
Nucl. Phys. **A529** (1991) 289.

[5] S.J. Krieger, P. Bonche, M.S. Weiss, J. Meyer, H. Flocard and P.-H. Heenen
Nucl. Phys. **A542** (1992) 43.

[6] R.B. Firestone and B. Singh
"Table of superdeformed Nuclear Bands", LBL Report No.LBL-35916, unpublished, and references therein.

[7] J.R. Hughes et al.,
Phys. Rev. **C51** (1995) 447.

[8] L.P. Farris et al.,
Phys. Rev. **C51** (1995) R2288.

[9] I.M. Hibbert et al.,
Submitted to Phys. Rev. C.

[10] Y. Liang et al.,
Phys. Rev. **C46** (1992) R2136.

[11] J. Duprat et al.,
Proceedings of the International Conference on the Future of Nuclear Spectroscopy, Crete, Greece (1993) p199.

[12] M.J. Joyce et al.,
Phys. Lett. **B340** (1994) 150.

[13] M.P. Carpenter et al.,
Phys. Rev. **C51** (1995) 2400.

[14] M.J. Joyce et al.,
Phys. Rev. Lett. **71** (1993) 2176.

[15] J. Duprat et al.,
Phys. Lett. **B341** (1994) 6.

[16] S. Bouneau et al.,
Phys. Rev. **C53** (1996) R9.

[17] P.J. Nolan
Nucl. Phys. **A520** (1990) 657c.
F.A. Beck
Proceedings of the First European Biennial Workshop on Nuclear Physics, Megève, ed. by D. Guinet and J.R. Pizzi (1991) p365.
N. Redon and the EUROGAM Collaboration
Proceedings of the XXXIII International Winter Meeting on Nuclear Physics, Bormio, ed. by I. Iori (1995) 1 and references therein.

[18] L. Ducroux et al.,
Z. Phys. **A352** (1995) 13.

[19] S. Flibotte, U.J. Hüttmeier, P. Bednarczyk, G. De France, B. Haas, P. Romain, Ch. Theisen, J.P. Vivien and J. Zen
Nucl. Inst. and Meth. in Phys. Res. **A320** (1992) 325.

[20] B. Crowell, M.P. Carpenter, R.G. Henry, R.V.F. Janssens, T.L. Khoo, T. Lauritsen and D. Nisius
Nucl. Inst. and Meth. in Phys. Res. **A355** (1995) 575.

[21] J.M. Lagrange, M. Pautrat, J.S. Dionisio, Ch. Vieu and J. Vanhorenbeeck
Nucl. Phys. **A530** (1991) 437.

[22] J.A. Becker et al.,
Phys. Rev. **C46** (1992) 889.

[23] C.S. Wu, L. Cheng, C.Z. Lin and J.Y. Zeng
Phys. Rev. **C45** (1992) 2507.

[24] B. Gall, P. Bonche, J. Dobaczewski, H. Flocard and P.-H. Heenen
Z. Phys. **A348** (1994) 183.

[25] F.S. Stephens et al.,
Phys. Rev. Lett. **65** (1990) 301.

[26] J. Terasaki, P.-H. Heenen, P. Bonche, J. Dobaczewski and H. Flocard
Nucl. Phys. **A593** (1995) 1.

[27] P. Willsau et al.,
Z. Phys. **A344** (1993) 351.

[28] J. Meyer, P. Bonche, M.S. Weiss, J. Dobaczewski, H. Flocard and P.-H. Heenen
Nucl. Phys. **A588** (1995) 597.

[29] S. Perries et al.,
to be published.

[30] M. Meyer, N. Redon, P. Quentin and J. Libert
Phys. Rev. **C45** (1992) 233.

[31] P.B. Semmes, I. Ragnarsson and S. Åberg
Phys. Lett. **B345** (1995) 185.

Table Caption

Table 1 γ-ray energies (in keV) of the six SD bands in ^{193}Pb. The new γ-rays are labelled by $*$.

Table 2 Values of the intrinsic spin on the z-axis, $\langle s_z \rangle$, and g_K for the neutron [512]5/2 and [624]9/2 configurations, extracted from Hartree-Fock + BCS calculations using the parametrizations (HF (SkM*)) SkM* [29] and (HF (SIII)) SIII [30] of the Skyrme force, and Woods-Saxon (WS) wave functions of Semmes et al. [31] calculated with $g_s^{\rm eff} = 0.7\, g_s^{\rm free}$ and $g_s^{\rm eff} = 0.9\, g_s^{\rm free}$ and experimental value of g_K measured in ^{193}Hg [14] and ^{193}Pb (this work).

Figure Caption

Figure 1 Background-substracted triple-gated spectra for the six SD bands of ^{193}Pb. SD band transitions are labeled by : ■ band 1, □ band 2, • band 3, ○ band 4, ▼ band 5, △ band 6. Low-lying yrast transitions are denoted by y. In these spectra, all indicated transitions are used as gates except the 708 keV for band 1, the 610, 649 and 690 keV for band 2, the 251, 673 and 707 keV for band 3, the 273, 676 and 709 keV for band 4, the 213, 254, 596, 632 and 667 keV for band 5 and 234, 684 and 717 keV for band 6. Insets give the relative transition intensities, corrected for E2 internal conversion, as a percentage of the largest peak intensity in the band.

Figure 2 Experimental $\Im^{(2)}$ dynamical moments of inertia as a function of the rotational frequency for the six SD bands in ^{193}Pb (■ band 1, □ band 2, • band 3, ○ band 4, ▼ band 5, △ band 6) and for the yrast SD band in ^{192}Pb (dashed line).

Figure 3 Experimental routhians as a function of the rotational frequency for the six SD bands observed in ^{193}Pb (■ band 1, □ band 2, • band 3, ○ band 4, ▼ band 5, △ band 6).

Figure 4 a) CHFBLN single-neutron and b) CHFBLN quasineutron routhians as a function of the rotational frequency. (π,α) : solid = (+,+), dashed = (+,-), dash-dotted = (-,+), dotted = (-,-). h : hole excitation, p : particle excitation.

Figure 5 Incremental alignments as a function of the rotational frequency for bands 3 (•) and 4 (○) in ^{193}Pb and bands 2 (◇) and 3 (◆) in ^{191}Hg relative to band 1 in ^{194}Pb and ^{192}Hg respectively.

Figure 6 Low energy part of the background-substracted triple-gated spectrum for band 6 shown in Figure 1. (▼ band 5, △ band 6, * interband dipole transitions).

Figure 7 Level scheme for the pair of signature partner bands. The energies of the dipole transitions are assigned within 0.5 keV uncertainty.

Figure 8 The extracted $(g_K - g_R)K\, f(I,K)/Q_0$ ($f(I,K) = \langle IK10|I-1K\rangle/\langle IK20|I-2K\rangle$) values for four SD states in band 6 as a function of their evaluated spins. The theoretical limits for the neutron [512]5/2 and [624]9/2 configurations, using $g_s^{\rm eff} = 0.9\, g_s^{\rm free}$, are indicated by full lines for the experimental value $Q_0 = 20 \pm 4$ eb of ^{194}Pb, and dotted and dashed lines for the predicted values of ^{192}Pb $Q_0 = 18.4$ eb and $Q_0 = 16.7$ eb respectively.

Band 1 (27/2)	Band 2 (17/2)	Band 3 (21/2)	Band 4 (23/2)	Band 5 (17/2)	Band 6 (19/2)
277.2(3)	190.5(5)	250.6(5)*	273.0(7)*	212.9(6)	234.1(7)
317.2(3)	232.5(4)	291.5(3)	313.7(6)	254.5(7)	275.8(6)
357.3(3)	275.0(4)	332.0(3)	352.9(3)	295.4(6)	315.9(6)
397.4(3)	317.9(4)	371.8(3)	391.6(5)	335.7(7)	355.7(6)
437.6(3)	360.9(3)	411.2(4)	429.8(4)	375.0(5)	394.4(6)
477.3(4)	403.6(4)	450.4(4)	466.9(4)	413.6(6)	432.9(6)
517.0(5)	445.7(4)	488.8(4)	503.7(5)	451.6(5)	470.4(6)
555.8(4)	488.3(5)	526.5(5)	539.9(6)	488.8(7)	507.5(6)
594.5(6)	527.5(6)	563.1(5)	575.0(5)	526.2(8)	543.6(6)
632.5(6)	569.8(7)*	600.1(5)	609.1(5)	561.5(6)*	579.4(7)
671.0(6)*	610.2(8)*	636.6(6)*	643.0(6)*	596.5(10)*	614.9(8)*
708.2(8)*	649.5(8)*	672.7(6)*	676.4(6)*	632.0(8)*	649.3(9)*
	689.8(8)*	707.3(6)*	709.3(6)*	667.0(8)*	683.7(9)*
					717.5(10)*

Table 1 Ducroux et al, PRC

		[512]5/2	[624]9/2
$\langle S_z \rangle$	HF (SkM*)	0.4259	0.4614
	HF (SIII)	0.4625	0.4630
	WS	0.45	0.46
g_K $(0.7 g_s^{free})$	HF (SkM*)	−0.456	−0.275
	HF (SIII)	−0.495	−0.276
	WS	−0.482	−0.274
g_K $(0.9 g_s^{free})$	HF (SkM*)	−0.587	−0.353
	HF (SIII)	−0.637	−0.354
	WS	−0.620	−0.352
g_K (exp.)		-0.65 ± 0.14	-0.39 ± 0.12

Table 2 Ducroux et al, PRC

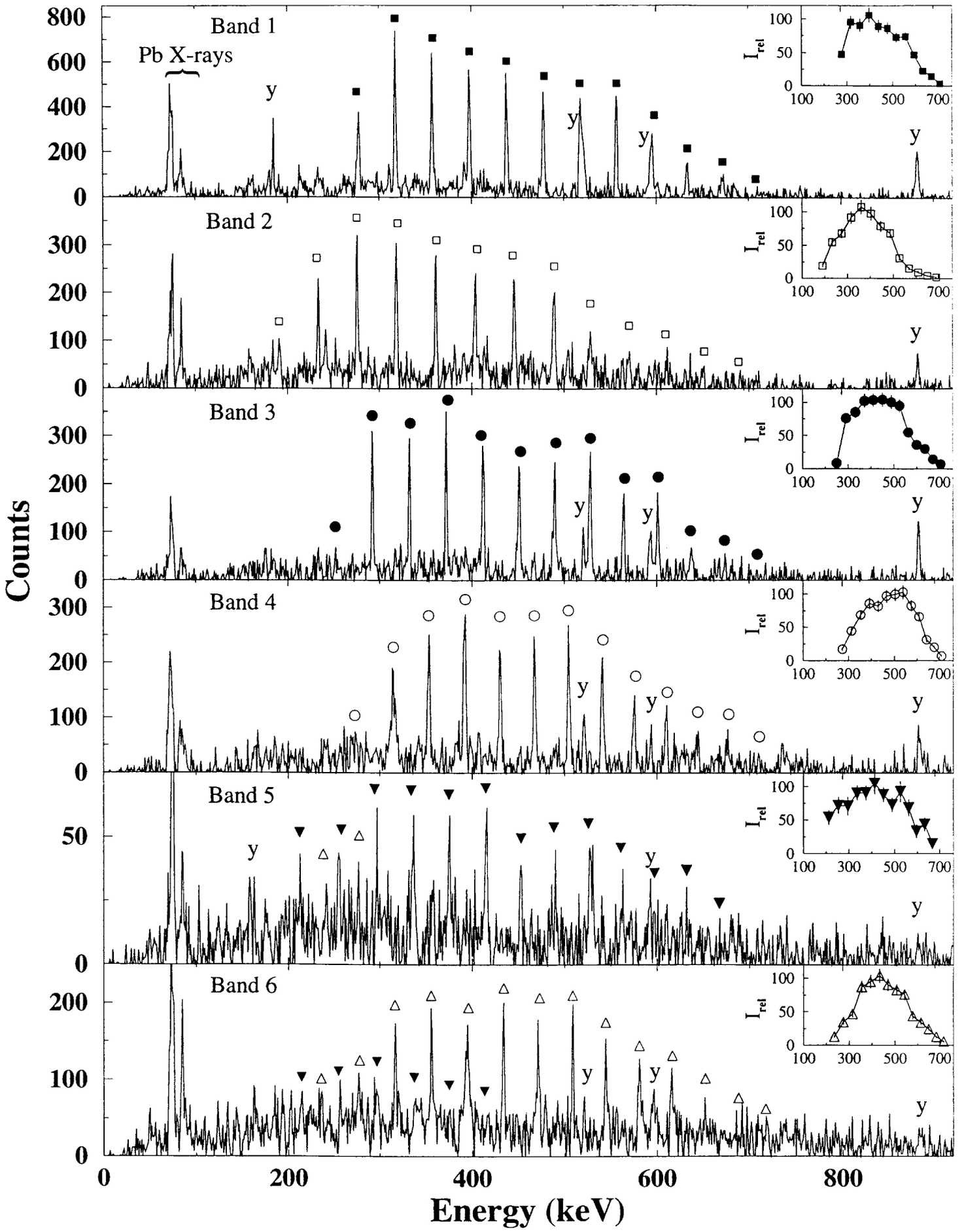

Fig. 1 Ducroux et al, PRC

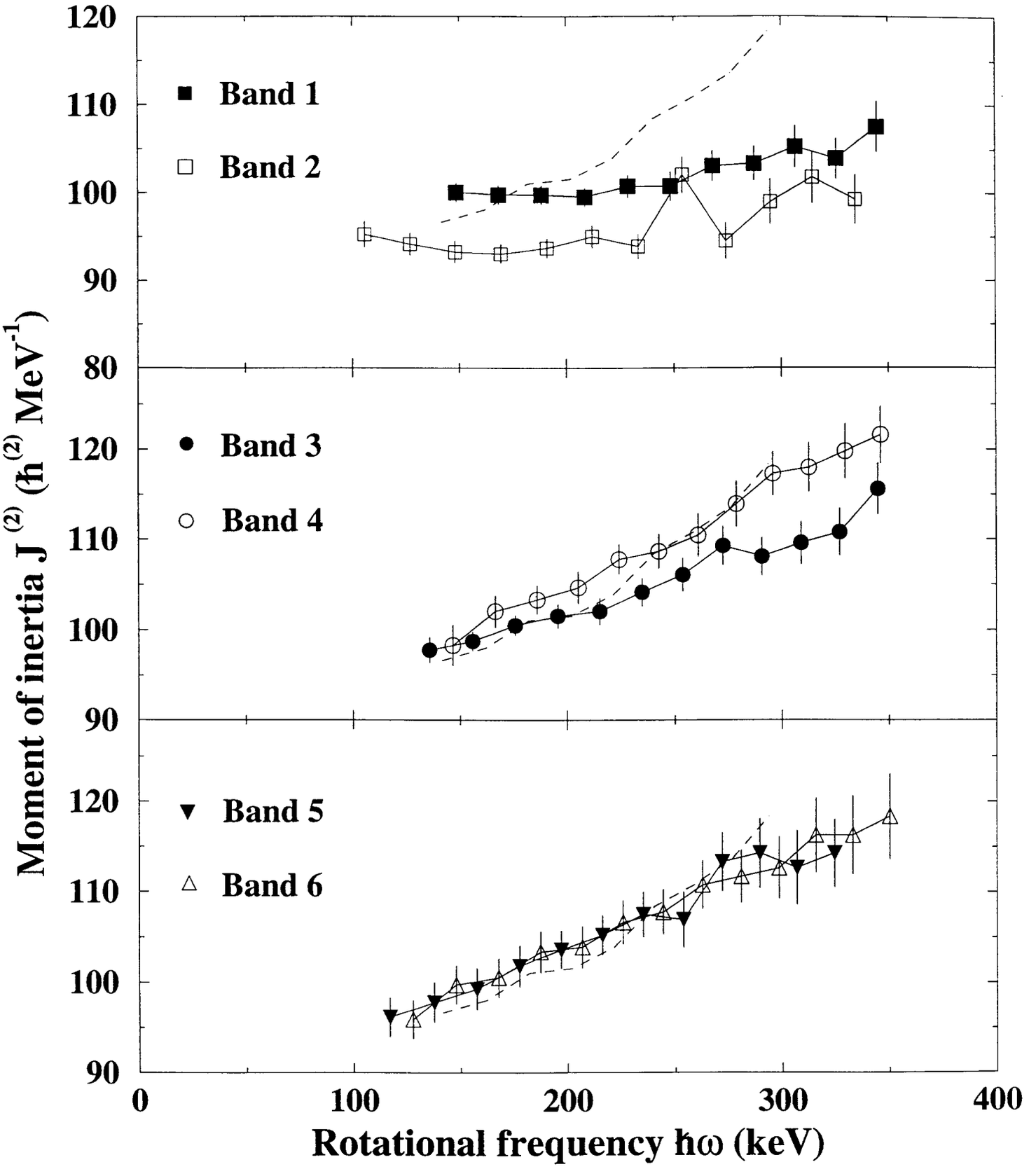

Fig. 2 Ducroux et al. PRC

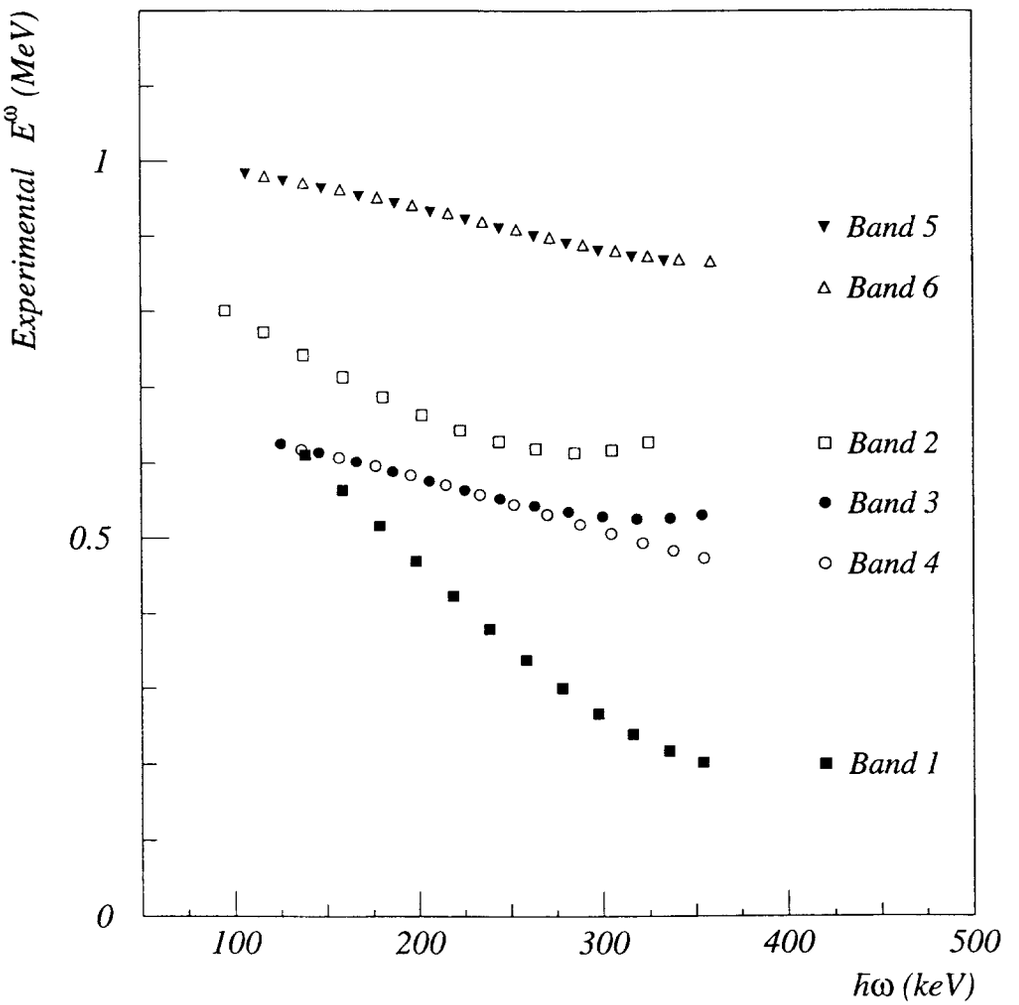

Fig. 3 Ducroux et al, PRC

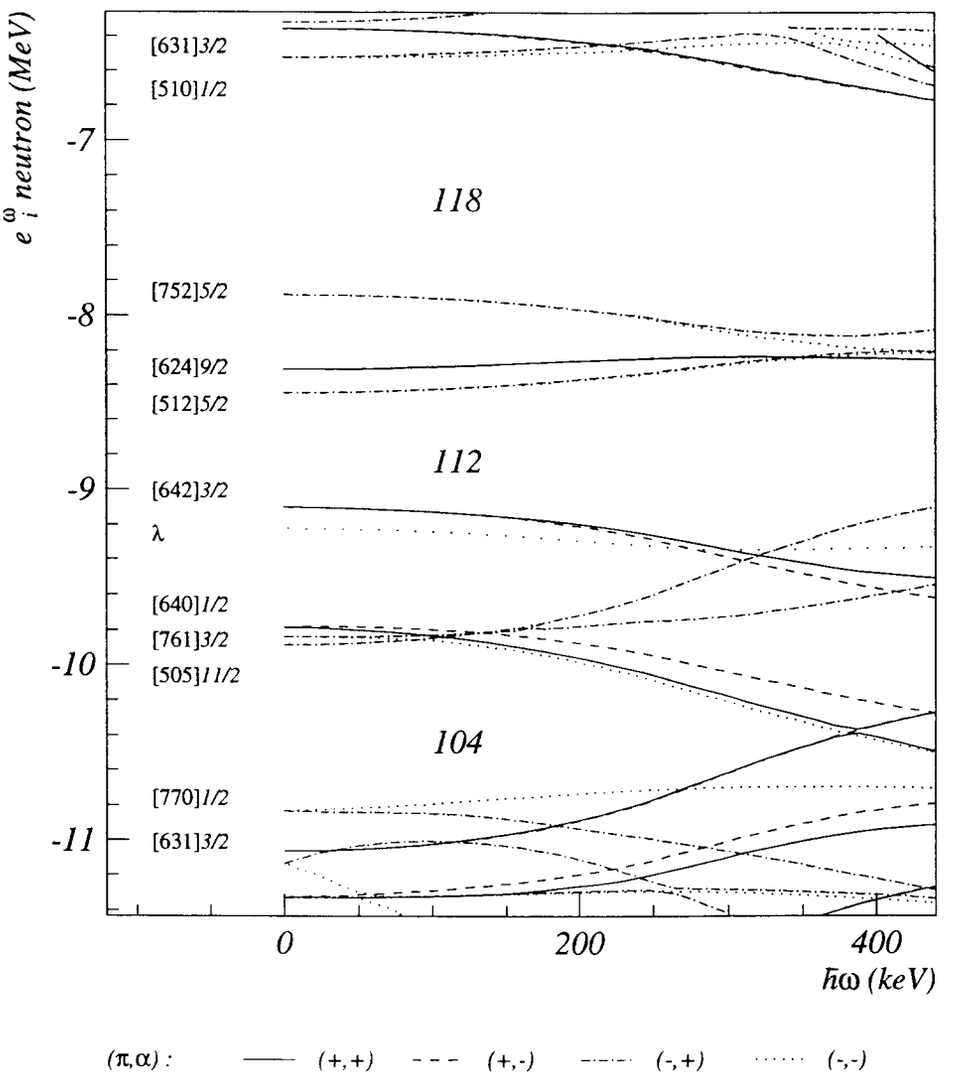

Fig. 4a Ducroux et al, PRC

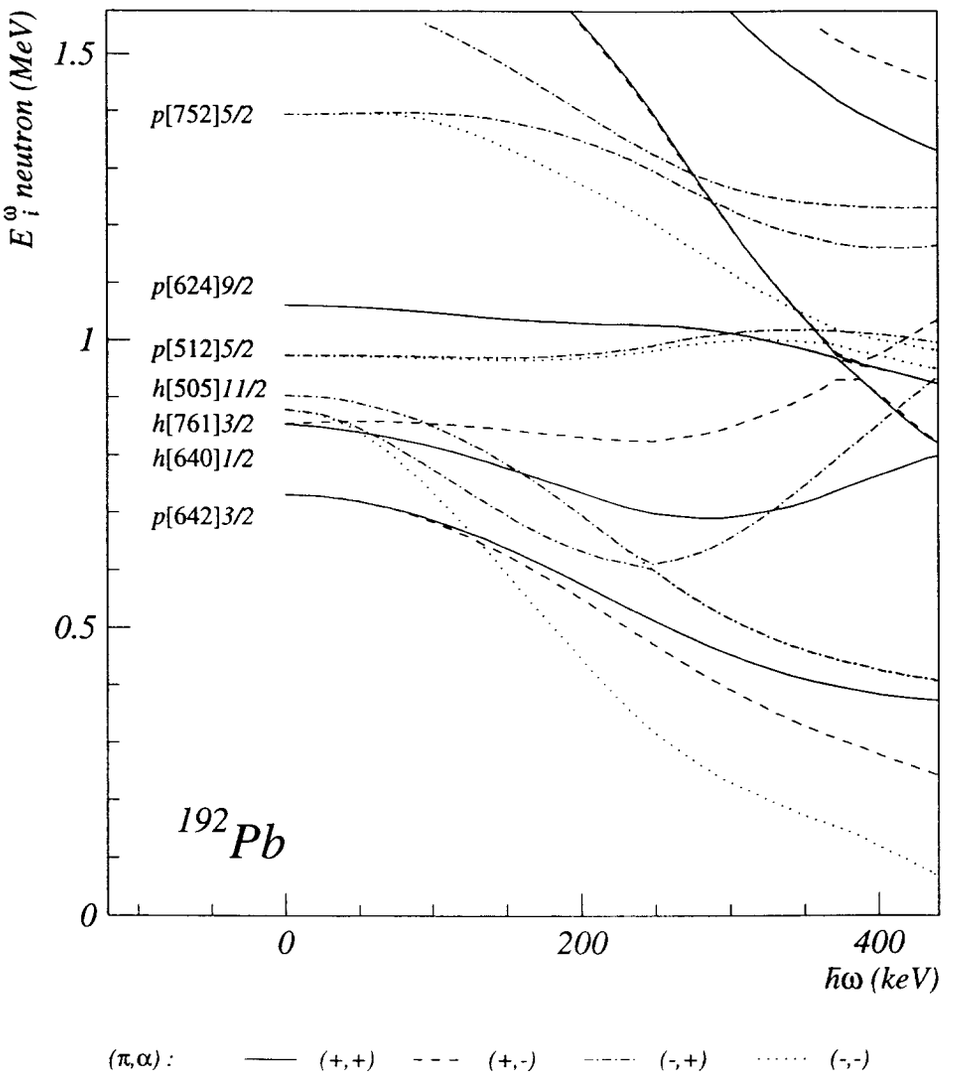

Fig. 4b Ducroux et al, PRC

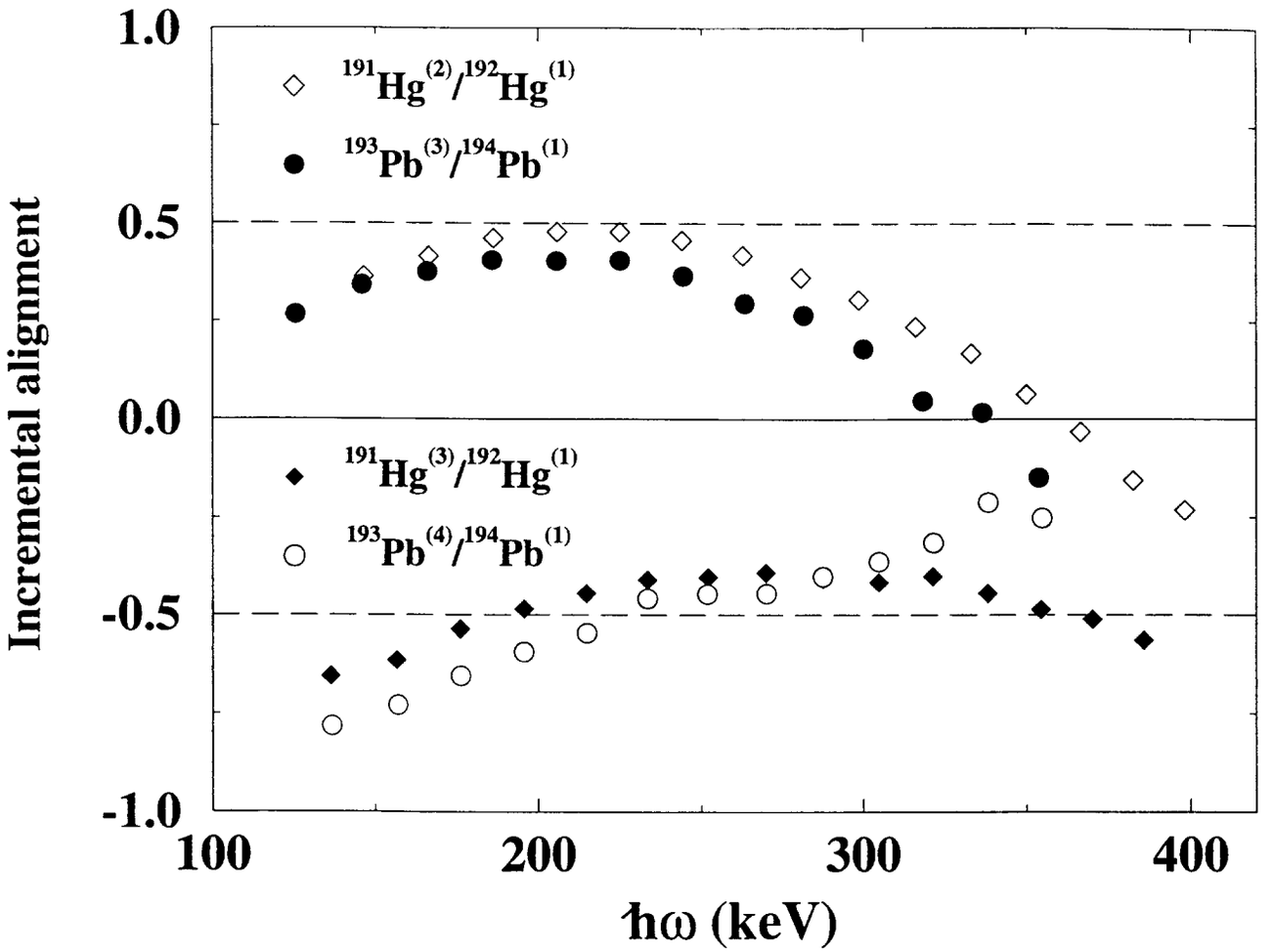

Fig. 5 Ducroux et al, PRC

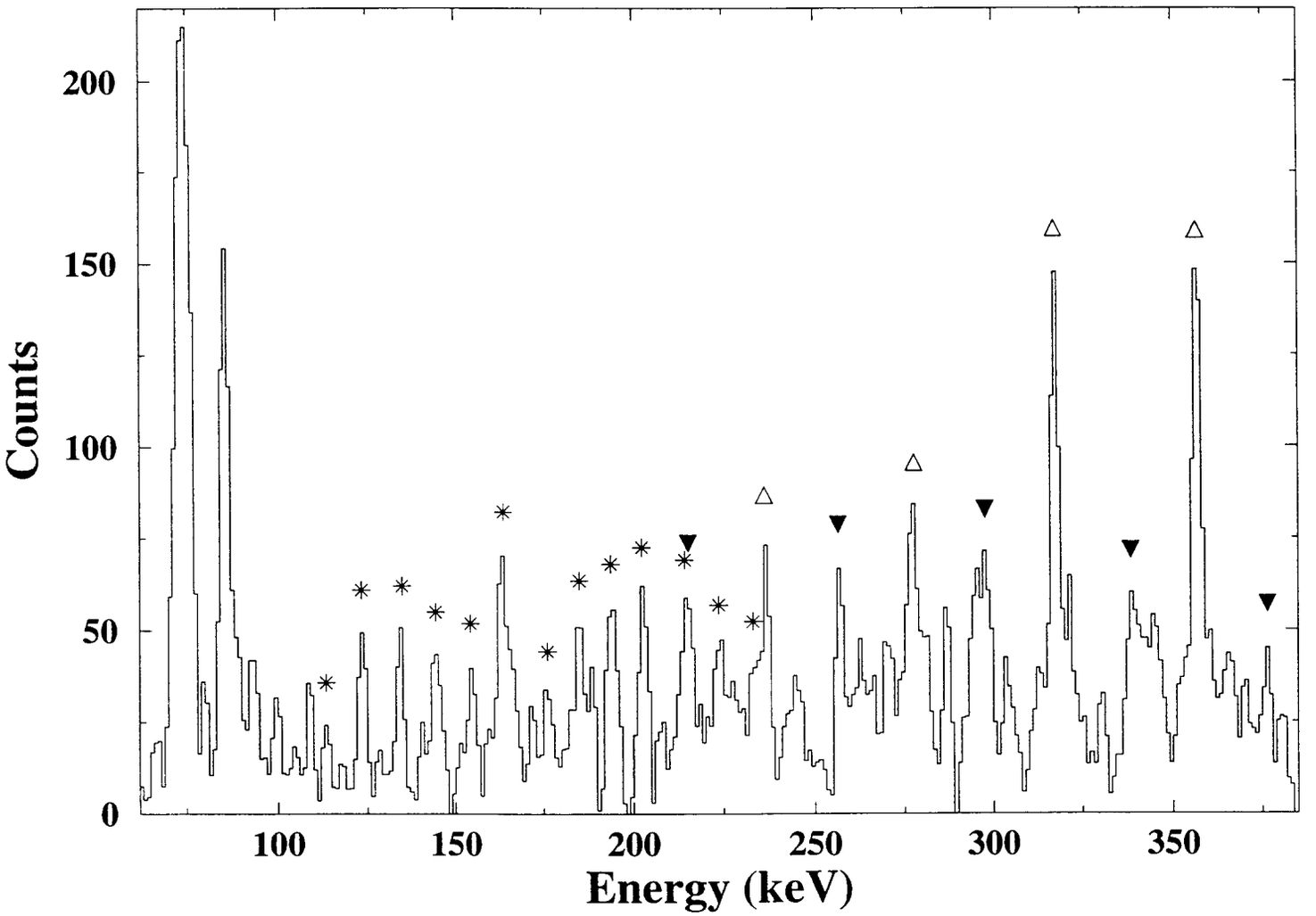

Fig. 6 Ducroux et al, PRC

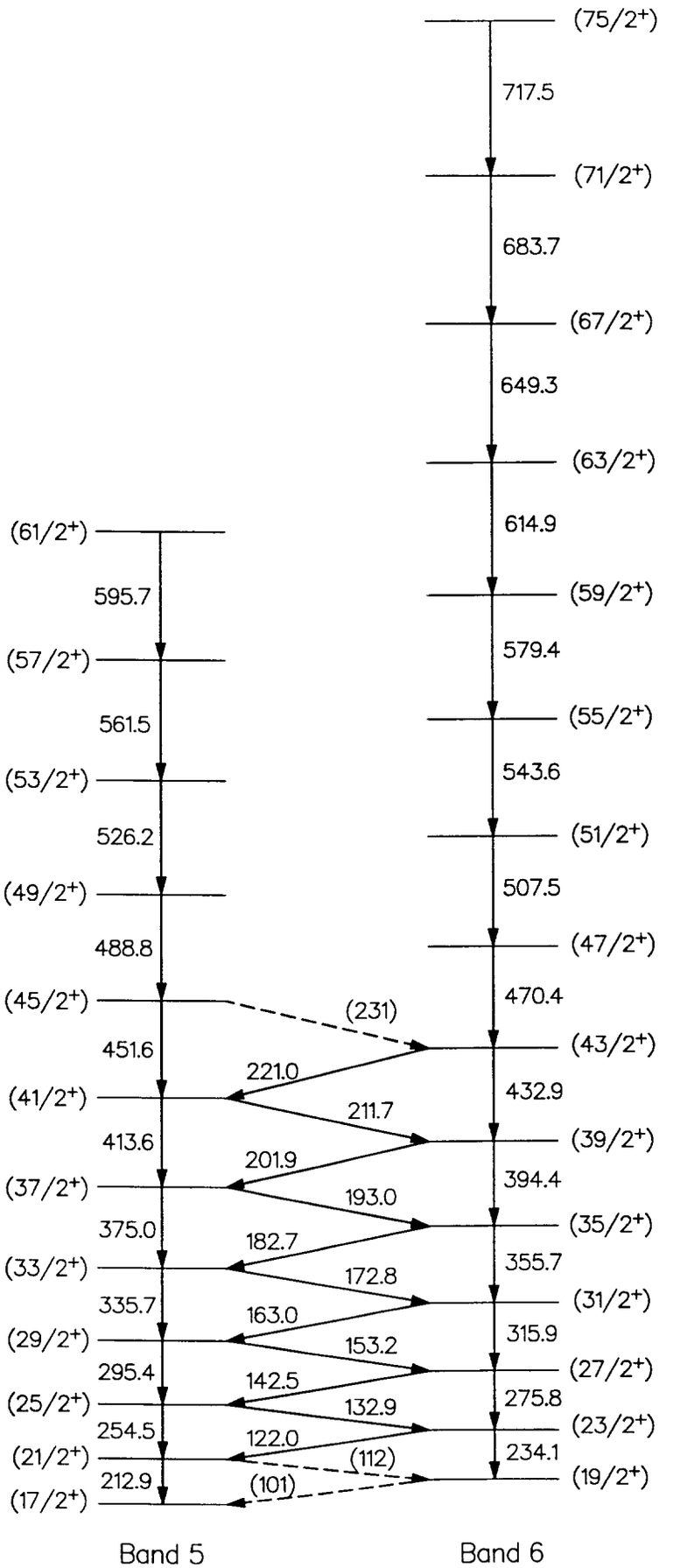

Fig. 7 Ducroux et al. PRC

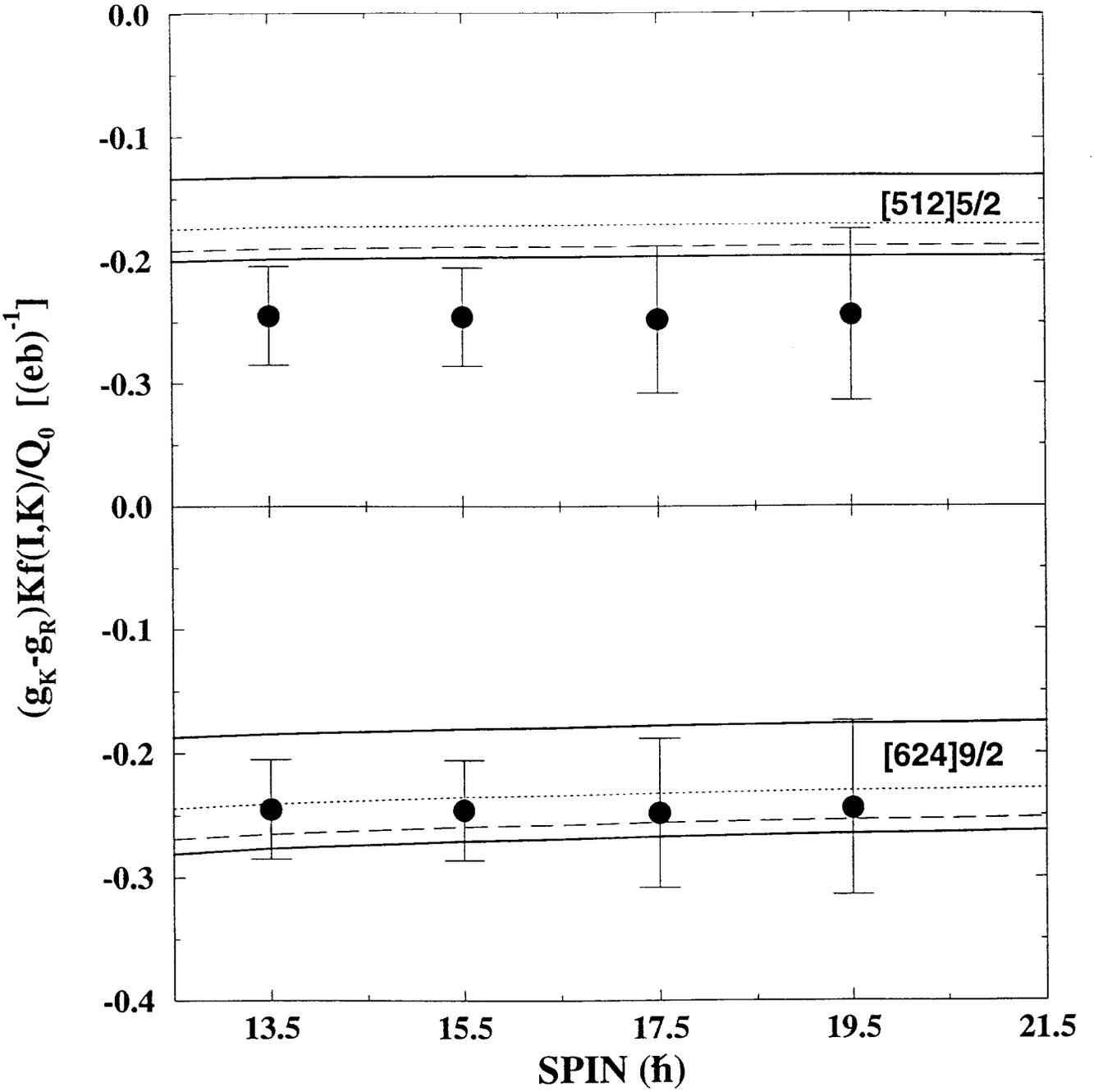

Fig. 8 Ducroux et al, PRC